PHYSICAL REVIEW B **92**, 035432 (2015)

Optical emission from SiO_2-embedded silicon nanocrystals: A high-pressure Raman and photoluminescence study

J. Ibáñez,[1,*] S. Hernández,[2] J. López-Vidrier,[2] D. Hiller,[3] S. Gutsch,[3] M. Zacharias,[3] A. Segura,[4] J. Valenta,[5] and B. Garrido[2]

[1]*Institute of Earth Sciences Jaume Almera, ICTJA-CSIC, Lluís Solé i Sabarís s/n, 08028 Barcelona, Catalonia, Spain*

[2]*MIND-IN$_2$UB, Departament d'Electrònica, Universitat de Barcelona, Martí i Franquès 1, 08028 Barcelona, Catalonia, Spain*

[3]*IMTEK, Faculty of Engineering, Albert-Ludwigs-University Freiburg, Georges-Köhler-Allee 103, D-79110, Freiburg, Germany*

[4]*Departamento de Física Aplicada-ICMUV-MALTA Consolider Team, Universitat de València, 46100 Burjassot, València, Spain*

[5]*Faculty of Mathematics and Physics, Charles University, Ke Karlovu 3, 121 16 Prague 2, Czech Republic*

(Received 24 March 2015; revised manuscript received 30 June 2015; published 27 July 2015)

We investigate the optical properties of high-quality Si nanocrystals (NCs)/SiO_2 multilayers under high hydrostatic pressure with Raman scattering and photoluminescence (PL) measurements. The aim of our study is to shed light on the origin of the optical emission of the Si NCs/SiO_2. The Si NCs were produced by chemical-vapor deposition of Si-rich oxynitride (SRON)/SiO_2 multilayers with 5- and 4-nm SRON layer thicknesses on fused silica substrates and subsequent annealing at 1150 °C, which resulted in the precipitation of Si NCs with an average size of 4.1 and 3.3 nm, respectively. From the pressure dependence of the Raman spectra we extract a phonon pressure coefficient of $8.5 \pm 0.3\,\mathrm{cm}^{-1}$/GPa in both samples, notably higher than that of bulk Si ($5.1\,\mathrm{cm}^{-1}$/GPa). This result is ascribed to a strong pressure amplification effect due to the larger compressibility of the SiO_2 matrix. In turn, the PL spectra exhibit two markedly different contributions: a higher-energy band that redshifts with pressure, and a lower-energy band which barely depends on pressure and which can be attributed to defect-related emission. The pressure coefficients of the higher-energy contribution are (-27 ± 6) and (-35 ± 8) meV/GPa for the Si NCs with a size of 4.1 and 3.3 nm, respectively. These values are sizably higher than those of bulk Si (−14 meV/GPa). When the pressure amplification effect observed by Raman scattering is incorporated into the analysis of the PL spectra, it can be concluded that the pressure behavior of the high-energy PL band is consistent with that of the indirect transition of Si and, therefore, with the quantum-confined model for the emission of the Si NCs.

DOI: 10.1103/PhysRevB.92.035432 PACS number(s): 78.67.Bf, 78.30.Am, 74.62.Fj

I. INTRODUCTION

Silicon nanocrystals (Si NCs) are currently the subject of intense research due to their potential application as efficient all-silicon light emitters and absorbers for optoelectronics and photovoltaics. The interest in nanosized Si was first sparked by the discovery of room-temperature optical emission in porous Si [1,2], and was subsequently boosted by reports of highly efficient photoluminescence (PL) in Si nanostructures [3–6].

In spite of much effort to investigate the optical properties of nanosized Si, the actual origin of its strong PL signal is still under debate [7–10]. While many experimental works point toward strong luminescence due to quantum-confined excitons in Si nanostructures fabricated with different methods [8,11–14], others suggest that the PL emission arises from highly localized surface states [14–17]. Godefroo and co-authors, using PL measurements under high magnetic fields, showed that the optical emission of as-crystallized SiO_x/SiO_2 superlattices may be related to defects, whereas it becomes entirely originated by excitonic quantum confinement (QC) after H passivation [7]. Matrix-induced strain has also been shown to play an important role in the optical emission of matrix-embedded Si NCs relative to free-standing material [9].

High-pressure optical measurements provide a useful benchmark to investigate the fundamental properties of semiconductors and test the validity of theoretical models (for instance, density functional theory) for the calculation of their optical gaps, vibrational frequencies, or dielectric constants. In the particular case of nanosized Si, high-pressure PL studies are expected to provide relevant information about the origin of the optical emission. Cheong and co-authors [18] measured the hydrostatic pressure dependence of the PL signal of Si NCs/SiO_2 fabricated by ion-beam implantation, and found pressure coefficients of the order of −5 meV/GPa, inconsistent with the QC model. Hannah *et al.* [8] measured the pressure behavior of the PL emission in alkane-terminated colloidal Si NCs. These authors obtained pressure coefficients in close agreement with those of bulk Si (−14.1 meV/GPa) [19], concluding that the bright emission in their samples mainly arises from the indirect transition in Si. Recently, Goñi *et al.* [10] have used high-pressure experiments to investigate the origin of the visible emission in amorphous Si/SiO_x nanoparticles. Although these authors report PL pressure coefficients that are sizably lower than those of bulk Si, they still conclude that the strong PL signal in their samples is determined by QC, which is supported by the fact that their experimental pressure coefficients seem to be systematically related to nanoparticle sizes and emission energies. Although structural information is crucial to understand the effect of hydrostatic pressure on the optical properties of the Si NCs, among the previous high-pressure studies only Ref. [8] presented structural data as a function of pressure. In that work it was found by means of high-pressure x-ray diffraction that the bulk modulus of their free-standing material is close to that of bulk Si, thus supporting their PL results.

*Corresponding author: jibanez@ictja.csic.es

In the present work we perform simultaneous Raman and PL measurements under high hydrostatic pressure on two different samples containing high-quality Si NCs/SiO_2 multilayers. The aim of our study is to shed light on the origin of the bright PL of the matrix-embedded Si NCs/SiO_2 system. The Raman spectra show that the phonon pressure coefficients of the Si NCs/SiO_2 are sizably larger than those of bulk Si, indicating that the NCs are subject to a strong pressure amplification effect as a consequence of the larger compressibility of the matrix. In turn, we find that the PL emission of the Si NCs can be separated in two different components: a higher-energy contribution exhibiting a strong redshift with pressure, and a lower-energy one which is much less sensitive to pressure. When the pressure amplification effect observed by Raman scattering is incorporated into the analysis of the pressure-dependent optical emission, it is found that the pressure behavior of the high-energy optical emission is consistent with that of the indirect transition of Si and therefore with the QC model, while the PL signal at lower energies can be attributed to defectlike emission.

II. EXPERIMENT

For this study, controlled-size, high-quality Si NCs were fabricated by depositing 100 silicon-rich oxynitride (SRON)/SiO_2 multilayers (MLs) at 375 °C on fused silica substrates by plasma-enhanced chemical vapor deposition (PECVD). Two different samples, labeled A and B, were studied. The thickness of the SiO_2 layers in both samples was kept constant at 2 nm, while the nominal thickness of the SRON layers was $t_{SRON} = 5$ nm in sample A and $t_{SRON} = 4$ nm in sample B, leading to a total sample thickness of 700 and 600 nm, respectively. In order to precipitate the Si excess within the SRON layers, the as-grown samples were annealed for 1 h at 1150 °C in a conventional furnace. In this way, Si NCs of average sizes $L = 4.1$ and 3.3 nm as determined by transmission electron microscopy (see Ref. [20] for details) were precipitated in samples A and B, respectively. Further details of the sample preparation can be found in Ref. [21].

The samples were mechanically polished down to $\approx 20\,\mu$m, and small flakes of around $50 \times 50\,\mu m^2$ [2] were subsequently detached from the polished material and loaded into a gasketed membrane diamond anvil cell (DAC) [22]. A 16:3:1 mixture of methanol-ethanol-water was employed as pressure transmitting medium, and the applied pressure was evaluated with the ruby fluorescence method [23].

Photoluminescence and Raman spectra were simultaneously acquired, up to ~5 GPa, with a Horiba Jobin-Yvon LabRam spectrometer coupled to a high-sensitive CCD detector. The second harmonic of a continuous-wave Nd:YAG laser ($\lambda = 532$ nm) was employed to excite the samples for both techniques. The excitation radiation was focused with a ×50 long-working distance objective, and the optical emission and Raman-scattering signal were collected in backscattering geometry with the same objective. Two different diffraction gratings were used for each type of measurement: 300 grooves/mm for PL, and 1800 grooves/mm for the Raman measurements.

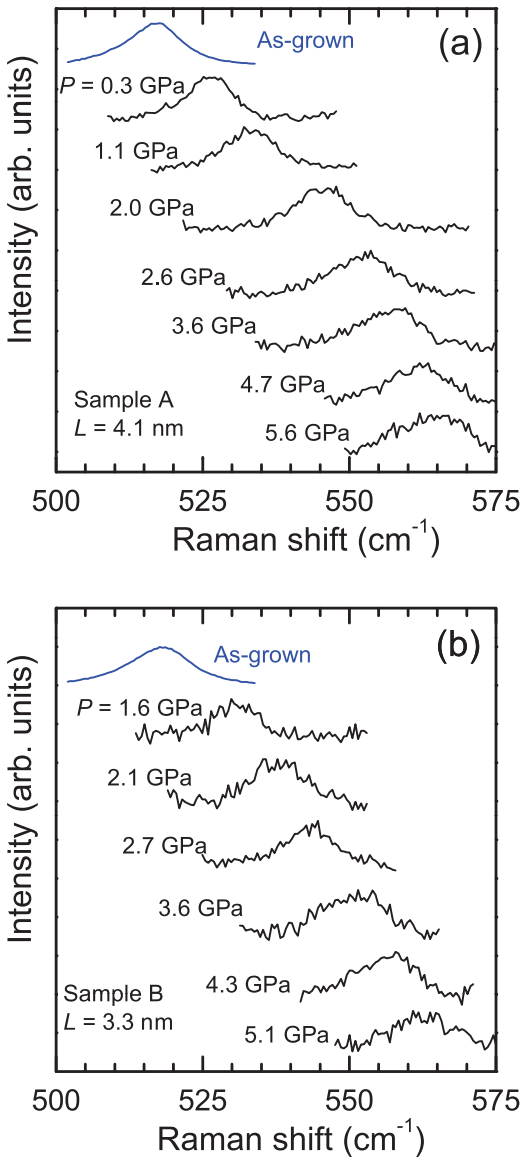

FIG. 1. (Color online) Raman spectra up to ~5 GPa of multilayered Si NCs embedded in a SiO_2 matrix with a NC size $L = 4.1$ nm (sample A, upper panel) and $L = 3.3$ nm (sample B, bottom panel). The top spectra (in blue) correspond to the as-grown samples, before the mechanical polishing for the high-pressure experiments.

III. RESULTS AND DISCUSSION

A. Raman scattering in Si/SiO_2: Pressure behavior

Figures 1(a) and 1(b) show the spectral region corresponding to the first-order optical phonons of crystalline Si as obtained by high-pressure Raman-scattering measurements on samples A and B, respectively. In both figures we have also included Raman spectra corresponding to the as-grown structures outside the DAC, before the mechanical polishing of the substrates. The ambient-pressure Raman spectra of these Si NCs have been discussed in detail elsewhere [20]. In Fig. 1, in order to isolate the Raman signal corresponding to crystalline Si, the contributions from the amorphous phases were carefully subtracted using a second-order polynomial. In this way, a clear Raman feature arising from the first-order

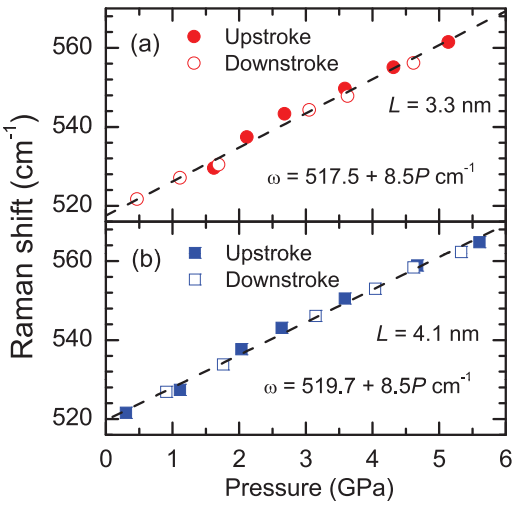

FIG. 2. (Color online) Pressure dependence of the frequency of the first-order optical phonon of Si in the two Si NCs/SiO_2 samples studied in this work. The dashed lines are linear fits to the experimental data.

optical phonons of nanocrystalline Si is clearly visible for both samples at all the explored pressures. The Raman spectra in Figs. 1(a) and 1(b) correspond to the upstroke cycle, up to ∼5 GPa. As can be seen in both figures, the Raman peaks exhibit a pronounced shift to higher frequencies with increasing pressure. This trend is completely reversed in the downstroke cycle (not shown). Above ∼5 GPa, a sizable intensity reduction of the Raman peaks was observed, accompanied by a decrease of the optical emission (see discussion of the PL data below).

Figure 2 shows the frequency of the first-order optical phonons in the two Si NCs/SiO_2 samples (A and B) as a function of applied pressure. Data obtained in the upstroke and downstroke cycles have been included in the two plots, both of which display a clear linear pressure dependence. From a linear fit to the experimental data, linear pressure coefficients $d\omega_{LO}^{NC}/dP$ equal to $8.5 \pm 0.3\,cm^{-1}$/GPa are obtained in both samples. Thus, we conclude that the experimental pressure coefficients in the Si NCs embedded in a SiO_2 matrix are significantly larger than those reported for bulk Si ($d\omega_{LO}^{bulk}/dP = 5.1\,cm^{-1}$/GPa) [24].

Increased phonon pressure coefficients have also been measured in other Si nanostructures. For instance, increased phonon pressure coefficients of $6.1\,cm^{-1}$/GPa were measured in Si nanowires (NWs) by Khachadorian and co-workers [25]. These authors explained their results in terms of a larger compressibility (lower bulk modulus) of the Si NWs in relation to bulk material as a consequence of an expansion of the lattice parameter. Note that, instead, decreased compressibilities are measured in Si NWs with reduced lattice parameter [26]. The results of Khachadorian *et al.* [25] can be compared to those obtained in porous Si, where a sizable expansion of the lattice parameter [27,28] and increased phonon pressure coefficients ($7.4\,cm^{-1}$/GPa, see for instance Ref. [29]) are typically reported.

However, in the case of the Si NCs/SiO_2 MLs studied in the present work, XRD measurements at $P = 0$ reveal that the ambient-pressure lattice parameter of Si is contracted in relation to bulk Si, and decreases with the crystalline size of the NCs [20]. Thus, according to the results of Refs. [25,26], our Si NCs/SiO_2 system should exhibit decreased compressibilities and reduced phonon pressure coefficients. Ambient-pressure Raman-scattering measurements also show that these Si NCs are subject to a sizable degree of compressive strain [20], which can be attributed to a compression effect of the SiO_2 matrix onto the NCs.

The previous considerations (i.e., observation of decreased lattice parameters and matrix-induced compression at $P = 0$) lead us to conclude that the large phonon pressure coefficients measured in our samples originate from a strong matrix-induced pressure amplification effect. Owing to the larger compressibility of the SiO_2 matrix (∼$0.027\,GPa^{-1}$) [30] relative to Si (∼$0.01\,GPa^{-1}$ in bulk samples) [24], the NCs may be subject to an effective pressure which is enhanced in relation to the applied (hydrostatic) pressure. Similar observations have been reported in Ge NCs embedded into SiO_2 [31] and also in thin layers grown on more compressible substrates (see for instance the recent high-pressure Raman scattering study on InGaN/Si(111) epilayers) [32]. In the particular case of the present work, strong Si-O covalent bonding at the NC-matrix interface is necessary in order to have effective transmission of deformations from the matrix to the NCs.

To illustrate the effect of the matrix-induced pressure amplification on the phonon pressure coefficients of the NCs, we first realize that the pressure coefficients, to the first order of the strain and assuming the same compressibility for the NCs and bulk Si, are proportional to the pressure coefficient of the residual (hydrostatic) strain ε in the NCs, which can be written in terms of the elastic properties of the matrix and the NCs [33]:

$$\frac{d\omega_{LO}^{NC}}{dP} = \frac{d\omega_{LO}^{bulk}}{dP} + \alpha\frac{d\varepsilon}{dP} \approx \frac{d\omega_{LO}^{bulk}}{dP} + \frac{\beta b_s}{3}\left(\frac{1}{B_0^m} - \frac{1}{B_0^{Si}}\right), \tag{1}$$

where b_s is the strain-shift coefficient for the optical phonon modes, B_0^m and B_0^{Si} represent the bulk modulus (i.e., the reciprocal of the compressibility) of the SiO_2 matrix and Si, respectively, and $d\omega_{LO}^{bulk}/dP = -b_s/3B_0^{Si}$ is the pressure coefficient of the optical first-order phonon of bulk Si [33], with $b_s \sim -1470\,cm^{-1}$ in the case of Si. In Eq. (1), α and β are phenomenological parameters that take into account the particular geometry and partial strain state of the geometrical configuration under study. An upper limit for $d\omega_{LO}^{NC}/dP$ can be readily obtained by assuming biaxially strained Si MLs, i.e., $\beta = 1$ in Eq. (1). The value thus obtained, using the bulk modulus values for Si and SiO_2, is ∼$13\,cm^{-1}$/GPa. As expected, this value is much larger than the experimental pressure coefficients measured in our samples. However, a value of β equal to 0.42, compatible with a partial relaxation and redistribution of the strain in the NCs, reproduces the experimental pressure coefficients measured in both samples.

Alternatively, the (hydrostatic) strain in the Si NCs at a given pressure value may be roughly evaluated by using the strain distribution inside a 0D dot embedded in a large matrix as given in Ref. [34], i.e., $\varepsilon = (1/\gamma - 1)\varepsilon_m$, where $\varepsilon_m = a_i(P)/a_m(P) - 1$ is the pressure-dependent lattice mismatch between the inclusion (0D dot) and the matrix, and $(1/\gamma - 1)$

is a constant that depends on the bulk modulus and Poisson ratio of both the matrix and the 0D dot (see Ref. [34] for details). Note that, by taking the pressure derivative of ε_m in terms of the bulk moduli of the NC and the matrix, this model is basically Eq. (1) with $\beta = (1/\gamma - 1)$. Using the appropriate material parameters for Si and SiO_2, we estimate a value of $d\omega_{LO}^{NC}/dP \sim 7.5\,cm^{-1}/GPa$, which is only $\sim 1\,cm^{-1}/GPa$ below the experimental pressure coefficients measured in our samples ($\sim 8.5\,cm^{-1}/GPa$).

In spite of the large oversimplifications involved in the two previous models, they provide a reasonable approximation to explain the pressure behavior of the first-order optical phonons in the Si NCs/SiO_2 system, thus confirming that matrix-induced compression may be responsible for the increased phonon pressure coefficients measured in our samples.

B. High-pressure optical emission

The pressure amplification effect revealed by the Raman measurements is expected to have an important bearing on the pressure dependence of the PL emission of the Si NCs/SiO_2 MLs. We show in Figs. 3(a) and 3(b) PL spectra as a function of pressure, obtained in the upstroke cycle up to $\sim$5 GPa, for samples A and B, respectively. These spectra were obtained simultaneously to the Raman spectra discussed above by simply shifting the diffraction gratings. In the figure we have also included PL spectra of the as-grown samples, before the mechanical polishing of the SiO_2 substrates. It can be seen that the maximum of the optical emission at ambient pressure of the two as-grown samples is redshifted in relation to the first spectra (i.e., at the lowest hydrostatic pressures) acquired in the DAC experiments. This observation can be attributed to a partial relaxation of the built-in strains in the NCs induced by the mechanical polishing and, more importantly, to dislocations formed during the polishing of the samples, which may be expected to affect more strongly the larger NCs, giving rise to an overall blueshift of the optical emission.

As can be seen in Fig. 3, the PL signal of both samples display a two-band emission that redshifts with pressure. The intensity of the high-energy PL band (peak P1 in Fig. 3) is found to progressively decrease with pressure. At the highest applied pressures, the low-energy portion of the spectra (peak P2) dominates the optical emission in both samples. In the downstroke cycle, the PL signal of both samples was almost totally recovered. This is illustrated in Fig. 4 for the case of sample A. As depicted in this figure, the PL emission of the sample with $L = 4.1$ nm around $\sim$1 GPa is very similar in the upstroke and downstroke cycles. Similar results are found in both samples along the whole pressure range investigated.

The PL peak energy of bands P1 and P2 in both samples was evaluated with a line-shape fit analysis. For this purpose, two Gaussian peaks (as a function of photon energy) were employed, one per each contribution, P1 and P2. In Fig. 4 we show some examples of the line-shape fitting analyses for the particular case of sample A. As can be seen in the figure, good agreement between the calculated and the experimental profiles is found.

Figure 5 shows the PL peak energy E_{Si/SiO_2} for bands P1 and P2 in both samples as a function of hydrostatic pressure. In the case of sample B ($L = 3.3$ nm), given the low PL intensity of peak P1 at the highest hydrostatic pressures, the corresponding curve only includes data below $\sim$3 GPa. As can be seen in the figure, the peak energy and also the pressure behavior of the low-energy PL emission (peak P2) is very similar in samples A and B. A linear fit to the data gives a pressure coefficient of (-10 ± 2) meV/GPa in both structures, thus suggesting that this PL band is independent of size effects.

On the other hand, Fig. 5 clearly shows that the PL peak energy for band P1 is higher in sample B, which is consistent with the larger QC effects expected in this structure in relation to sample A. From a linear fit to the data for peaks P1 in both samples we extract the following pressure coefficients: $dE_{Si/SiO_2}/dP = (-27 \pm 6)$ meV/GPa in sample A, and $dE_{Si/SiO_2}/dP = (-35 \pm 8)$ meV/GPa in sample B. As

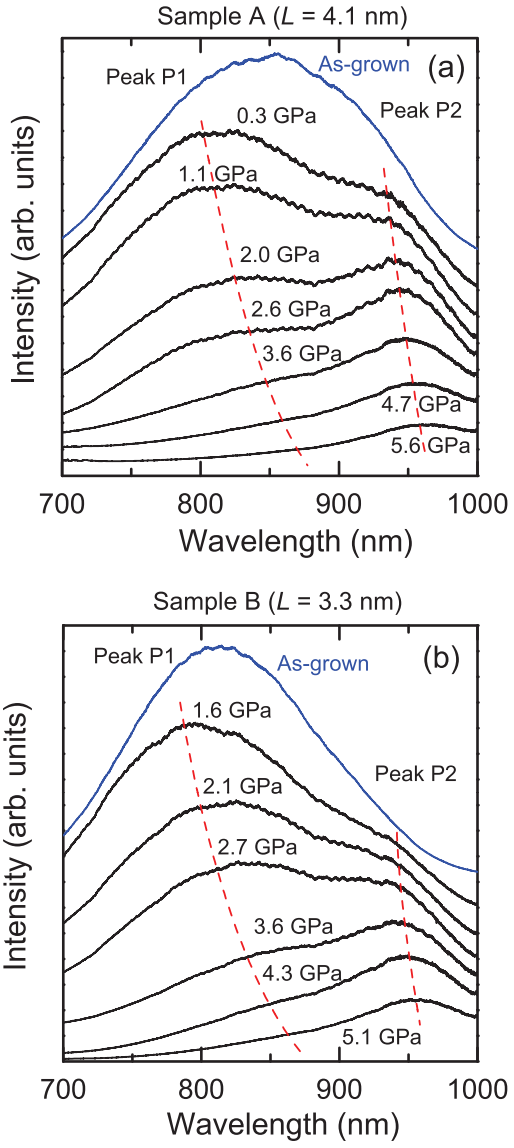

FIG. 3. (Color online) Photoluminescence (PL) spectra of two Si NC/SiO_2 samples with different NC sizes (L). (a) Sample A ($L = 4.1$ nm); (b) the PL spectra of sample B ($L = 3.3$ nm). The spectra on top (in blue) correspond to the as-grown samples before mechanical polishing for the high-pressure experiments.

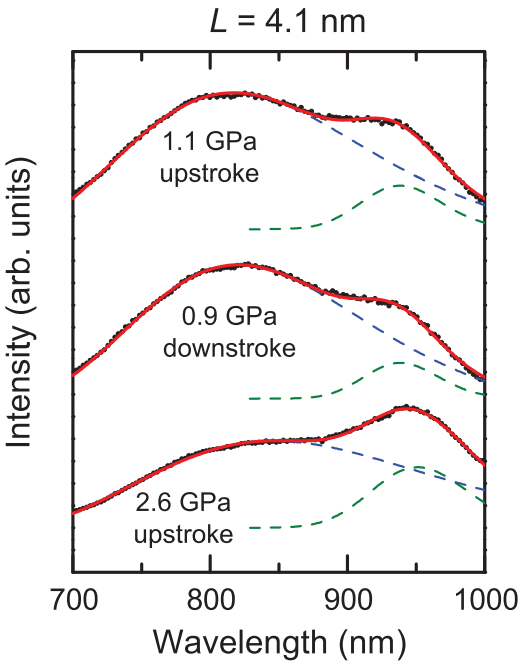

FIG. 4. (Color online) Selected photoluminescence (PL) spectra of sample A ($L = 4.1$ nm) obtained during the upstroke and downstroke cycles. The results of the line-shape fitting analysis of the PL spectra, carried out with two Gaussian functions (as a function of photon energy), are shown.

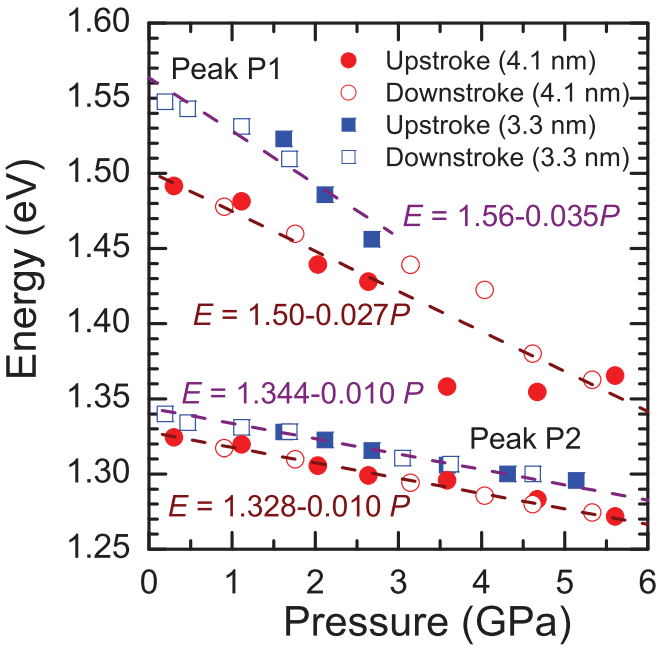

FIG. 5. (Color online) PL peak energies for the high-energy (peak P1) and low-energy (peak P2) optical emission of the two Si NC/SiO_2 samples studied in this work. The dots correspond to sample A (with a NC size $L = 4.1$ nm) and the squares to sample B ($L = 3.3$ nm).

occurred with the Raman-scattering data discussed above, these pressure coefficients are sizably larger (in absolute value) than those measured in bulk Si (-14.1 meV/GPa, see Ref. [19]). Again, we attribute this result to a pressure amplification effect induced by the more compressive matrix.

We would like to note the large error bars in the resulting PL pressure coefficients of peak P1 in both samples, which is a consequence of the observed PL intensity reduction of this band with increasing pressure. Within error bars, the two measured pressure coefficients are quite similar. This result does not alter the main conclusion of the present PL measurements, i.e., the fact that the experimental $dE_{Si/SiO_2}/dP$ values are much larger (in absolute value) than those of bulk Si.

The matrix-induced pressure amplification on the PL peak energies of bands P1 and also P2, relative to those expected in "free-standing" (i.e., not compressed by the matrix) Si NCs can be roughly estimated by using the following phenomenological (ad hoc) expression:

$$dE_{Si/SiO_2}/dP = \varphi_{amp} dE_{free}/dP \sim \frac{\left(d\omega_{LO}^{NC}/dP\right)}{\left(d\omega_{LO}^{bulk}/dP\right)}(dE_{free}/dP), \quad (2)$$

where E_{free} corresponds to the PL peak energy in free-standing material. In Eq. (2) the amplification factor φ_{amp} is simply evaluated in terms of the amplification of the phonon pressure coefficients in the Si NCs/SiO_2 MLs relative to bulk Si. Taking the experimental $d\omega_{LO}^{NC}/dP$ values measured above ($8.5\,cm^{-1}$/GPa in both samples) and that of bulk Si ($5.1\,cm^{-1}$/GPa), we obtain an amplification factor φ_{amp} equal to 1.67. Using this value in Eq. (2) together with the experimental $dE_{Si/SiO_2}/dP$ values for peaks P1 and P2 in samples A and B, we obtain the corresponding dE_{free}/dP values, which are shown in Table I.

In the case of peak P2, the resulting PL pressure coefficients in free-standing NCs are around -6 meV/GPa in both samples. This value is compatible with radiative emission from localized levels, which suggests that the low-energy emission in these NCs is mainly originated by defects, as for instance highly localized defects at the Si/SiO_2 interface [7]. Such interface states may be close to the band-gap edges of nanocrystalline Si and could partly follow the band-gap dependence of Si with NC size [7]. The fact that the intensity ratio between bands P2 and P1 is found to increase in the polished samples, relative to the as-grown material (see Fig. 3), seems to further support the conclusion that P2 may be related to defects. We would also like to note that the dE_{free}/dP values that we obtain for peak P2 are comparable to those measured in poorly crystalline samples, as for instance those produced by ion-beam implantation in Ref. [18], where pressure coefficients of -4 and -6 meV/GPa were measured. The similarity between those values and our present results for peak P2 may suggest that the PL emission in the ion-implanted samples [18] is actually originated by radiative defects.

In the case of the high-energy PL emission (peak P1), we find that the resulting pressure coefficients in "free-standing" NCs (see Table I) are not far from those of bulk Si ($dE_g/dP = -14.1$ meV/GPa). This suggests that peak P1 may be related to the indirect gap of Si. Very similar PL pressure coefficients, ranging from -14.2 to -21.1 meV/GPa, were reported by

TABLE I. Experimental peak energy (E_{PL}) at $P = 0$ and pressure coefficients ($dE_{Si/SiO_2}/dP$) for the PL peak energy of the high-energy optical emission (peak P1) and low-energy emission (peak P2) measured by high-pressure PL measurements in the two samples studied in this work. The fourth and seventh columns show the corresponding PL pressure coefficients (dE_{free}/dP), which have been recalculated phenomenologically to subtract the pressure amplification effect induced by the SiO_2 matrix. Values for bulk Si, as in Ref. [19], are also given.

	Peak P1			Peak P2		
Sample	$E_{PL}(P=0)$ (meV)	$dE_{Si/SiO_2}/dP$ (meV/GPa)	dE_{free}/dP (meV/GPa)	$E_{PL}(P=0)$ (meV)	$dE_{Si/SiO_2}/dP$ (meV/GPa)	dE_{free}/dP (meV/GPa)
A ($L = 4.1$ nm)	1500 ± 10	-27 ± 6	-16 ± 4	1328 ± 2	-10 ± 2	-6 ± 1
B ($L = 3.3$ nm)	1560 ± 10	-35 ± 8	-21 ± 6	1344 ± 2	-10 ± 2	-6 ± 1
Bulk Si [19]	1110 ± 2	–	-14.1 ± 0.6	–	–	–

Hannah *et al.* [8] in colloidal nanoparticles. Thus we can conclude that the high-energy optical emission in the Si NC/SiO_2 system mainly involves confined states associated to the X and Γ electronic states responsible for the indirect transition in bulk Si. In the case of our samples, the pressure behavior of the maximum of peak P1 is strongly affected by an amplification effect induced by the more compressible SiO_2 matrix, which explains the high $dE_{Si/SiO_2}/dP$ values measured in the present work.

Within this picture, the defect states related to peak P2 (see discussion above) may compete with the quantum-confined emission from the Si NCs, giving rise to the observed quenching of peak P1 with increasing pressure (Fig. 3), i.e., when the energy of the quantum-confined states responsible for peak P1 approaches that of the interface defect states. These observations also help us to better understand the effect of the mechanical polishing on the optical emission of the samples at ambient conditions (see Fig. 3). The mechanical polishing may introduce radiative defects (band P2) that compete with the optical emission from the NCs (band P1). Then, the intensity increase of band P2 together with the quenching of part of the high-energy contributions could explain, at least partially, the apparent blueshift of the PL spectra of both samples after the mechanical polishing. As a consequence of the intensity variations of bands P1 and P2, the spectra of the polished samples end up exhibiting two well-resolved PL bands, with an apparent blueshift of the high-energy contribution. As discussed above, the partial relaxation of the built-in strains in the NCs and an additional dislocation-induced quenching of the PL from the largest NCs would also contribute to the observed blueshifts.

Finally, we would like to remark that QC is not expected to strongly affect the $dE_{Si/SiO_2}/dP$ values measured in our Si NCs. The QC energy depends on pressure through volume and effective mass changes. With regard to the former, we follow the discussion of Cheong *et al.* [18] and evaluate the pressure coefficient (in free-standing NCs) of the confinement energy, $E_{conf} \sim E_{PL} - E_g$, where $E_g = 1.11$ eV [19] is the indirect band-gap of Si, with the expression $dE_{conf}/dP = (2/3)E_{conf}/B_0^{Si}$, where a simple cubic-box model for the quantum-confined carriers is assumed. Using the PL peak energies at $P = 0$, we obtain $E_{conf} \sim 380$ meV for sample A and $E_{conf} \sim 440$ meV for sample B. Inserting these values in the expression for dE_{conf}/dP, we obtain values between $2 - 3$ meV/GPa, which are of the order of the experimental errors associated to the high-pressure PL measurements. With regard to changes in E_{conf} due to the pressure dependence of the electron effective mass at the X valleys, there does not seem to be any experimental measurement of the corresponding pressure coefficient. Nevertheless, given that the electron effective mass determines (along with the dielectric constant) the ionization energy of shallow donors, its pressure coefficient is expected to be very small. This can be inferred, for instance, from the very low pressure coefficient of both the shallow donor ionization energy [35] and the dielectric constant [36] of bulk Si. These results, extrapolated to the case of the Si NCs, imply that the pressure behavior of the quantum-confined optical emission is not strongly affected by pressure-induced volume or electron effective-mass changes.

IV. CONCLUSIONS

We have performed Raman-scattering and PL measurements under high hydrostatic pressure on Si NC/SiO_2 MLs grown by PECVD. The aim of the present study is to obtain additional knowledge on the origin of the optical emission of the Si NCs embedded in SiO_2. The Raman-scattering experiments reveal that the phonon pressure coefficients of the Si NCs/SiO_2 (8.5 cm^{-1}/GPa) are sizably larger than those of bulk Si (5.1 cm^{-1}/GPa), which can be attributed to a pressure amplification effect on the NCs as a consequence of the larger compressibility of the SiO_2 matrix in relation to Si. For this purpose, strong covalent Si-O bonding at the NC-matrix interface would be required in order to have effective pressure transmission from the matrix to the less compressible NCs.

The PL spectra acquired as a function of pressure on the Si NCs display two different bands. The high-energy emission is found to strongly redshift with pressure (redshift of 27–35 meV/GPa), while the low-energy band is much less sensitive to pressure (redshift of 10 meV/GPa). By incorporating the pressure amplification effect observed by Raman scattering into the analysis of the PL data, we obtain PL pressure coefficients for the corresponding free-standing (matrix-free) NCs equal to -16 and -21 meV/GPa in the two samples investigated. These values agree well with values measured in colloidal NCs, and are not far from the PL pressure coefficient measured in bulk Si (-14.1 meV/GPa). Thus, we conclude that the pressure dependence of the high-energy optical emission of the Si NCs/SiO_2 is compatible with the indirect transition of Si, while the low-energy PL bands can be attributed to emission from defects.

ACKNOWLEDGMENTS

Work supported by the European Community's Seventh Framework Programme (FP7/2007-2013) under grant agreement No. 245977 (project NASCEnT). Financial support by the Spanish Government through projects LEOMIS (TEC2012-38540-C02-01) and MAT2012-38664-C02-02 is also acknowledged.

[1] L. T. Canham, Appl. Phys. Lett. **57**, 1046 (1990).
[2] V. Lehmann and U. Gösele, Appl. Phys. Lett. **58**, 856 (1991).
[3] S. H. Risbud, L. Liu, and J. F. Shackelford, Appl. Phys. Lett. **63**, 1648 (1993).
[4] T. S. Iwayama, S. Nakao, and K. Saitoh, Appl. Phys. Lett. **65**, 1814 (1994).
[5] Q. Zhang, S. C. Bayliss, and D. A. Hutt, Appl. Phys. Lett. **66**, 1977 (1995).
[6] P. Mutti, G. Ghislotti, S. Bertoni, L. Bonoldi, G. F. Cerofolini, L. Meda, E. Grilli, and M. Guzzi, Appl. Phys. Lett. **66**, 851 (1995).
[7] S. Godefroo, M. Hayne, M. Jivanescu, A. Stesmans, M. Zacharias, O. I. Lebedev, G. Van Tendeloo, and V. V. Moschchalkov, Nat. Nanotechnol. **3**, 174 (2008).
[8] D. C. Hannah, J. Yang, P. Podsiadlo, M. K. Y. Chan, A. Demortière, D. J. Gosztola, V. B. Prakapenka, G. C. Schatz, U. Kortshagen, and R. D. Schaller, Nano Lett. **12**, 4200 (2012).
[9] K. Kůsová, L. Ondič, E. Klimešová, K. Herynková, I. Pelant, S. Daniš, J. Valenta, M. Gallart, M. Ziegler, B. Hönerlage, and P. Gilliot, Appl. Phys. Lett. **101**, 143101 (2012).
[10] A. R. Goñi, L. R. Muniz, J. S. Reparaz, M. I. Alonso, M. Garriga, A. F. Lopeandia, J. Rodriguez-Viejo, J. Arbiol, and R. Rurali, Phys. Rev. B **89**, 045428 (2014).
[11] W. L. Wilson, P. F. Szajowski, and L. E. Brus, Science **262**, 1242 (1993).
[12] D. S. English, L. E. Pell, Z. H. Yu, P. F. Barbara, and B. A. Korgel, Nano Lett. **2**, 681 (2002).
[13] K. Kusova, O. Cibulka, K. Dohnalova, I. Pelant, J. Valenta, A. Fucikova, K. Zidek, J. Lang, J. Englich, P. Matejka, P. Stepanek, and S. Bakardjieva, ACS Nano **4**, 4495 (2010).
[14] M. Sykora, L. Mangolini, R. D. Schaller, U. Kortshagen, D. Jurbergs, and V. I. Klimov, Phys. Rev. Lett. **100**, 067401 (2008).
[15] A. Puzder, A. J. Williamson, J. C. Grossman, and G. Galli, Phys. Rev. Lett. **88**, 097401 (2002).
[16] G. Allan, C. Delerue, and M. Lannoo, Phys. Rev. Lett. **76**, 2961 (1996).
[17] K. Žídek, I. Pelant, F. Trojánek, P. Malý, P. Gilliot, B. Hönerlage, J. Oberlé, L. Šiller, R. Little, and B. R. Horrocks, Phys. Rev. B **84**, 085321 (2011).
[18] H. M. Cheong, W. Paul, S. P. Withrow, J. G. Zhu, J. D. Budai, C. W. White, and D. M. Hembree, Appl. Phys. Lett. **68**, 87 (1996).
[19] B. Welber, C. K. Kim, M. Cardona, and S. Rodríguez, Solid State Commun. **17**, 1021 (1975).
[20] S. Hernández, J. López-Vidrier, L. López-Conesa, D. Hiller, S. Gutsch, J. Ibáñez, S. Estradé, F. Peiró, M. Zacharias, and B. Garrido, J. Appl. Phys. **115**, 203504 (2014).
[21] A. M. Hartel, D. Hiller, S. Gutsch, P. Löper, S. Estradé, F. Peiró, B. Garrido, and M. Zacharias, Thin Solid Films **520**, 121 (2011).
[22] R. Le Toullec, J. P. Pinceaux, and P. Loubeyre, High Press. Res. **1**, 77 (1988).
[23] H. K. Mao, P. Bell, J. Shaner, D. Steinberg, J. Appl. Phys. **49**, 3276 (1978).
[24] S. Adachi, *Properties of Group-IV, III-V and II-VI Semiconductors* (John Wiley and Sons, NewYork, 2005), pp. 41–72.
[25] S. Khachadorian, K. Papagelis, H. Scheel1, A. Colli, A. C. Ferrari, and C. Thomsen, Nanotechnology **22**, 195707 (2011).
[26] Y. Wang, J. Zhang, J. Wu, J. L. Coffer, Z. Lin, S. V. Sinogeikin, W. Yang, and Y. Zhao, Nano Lett. **8**, 2891 (2008).
[27] K. Barla, R. Herino, G. Bomchil, J. C. Pfister, and A. Freund, J. Cryst. Growth **68**, 727 (1984).
[28] D. Bellet and G. Dolino, Thin Solid Films **276**, 1 (1996).
[29] D. Papadimitriou, Y. S. Raptis, A. G. Nassiopoulou, and G. Kaltsas, Phys. Status Solidi (a) **165**, 43 (1998).
[30] O. B. Tsiok, V. V. Brazhkin, A. G. Lyapin, and L. G. Khvostantsev, Phys. Rev. Lett. **80**, 999 (1998).
[31] L. Liu, Z. X. Shen, K. L. Teo, A. V. Kolobov, and Y. Maeda, J. Appl. Phys. **93**, 9392 (2003).
[32] R. Oliva, J. Ibáñez, R. Cuscó, A. Dadgar, A. Krost, J. Gandhi, A. Bensaoula, and L. Artús, Appl. Phys. Lett. **104**, 142101 (2014).
[33] J. S. Reparaz, A. Bernardi, A. R. Goñi, P. D. Lacharmoise, M. I. Alonso, M. Garriga, J. Novák, and I. Vávra, Appl. Phys. Lett. **91**, 081914 (2007).
[34] M. Yang, J. C. Sturm, and J. Prevost, Phys. Rev. B **56**, 1973 (1997).
[35] M. G. Holland and W. Paul, Phys. Rev. **128**, 30 (1962).
[36] G. A. Samara, Phys. Rev. B **27**, 3494 (1983).